Domain Patterns in the Microwave-Induced Zero-Resistance State

Ilya Finkler[1], Bertrand I. Halperin[1], Assa Auerbach[2], and Amir Yacoby[3],

[1]Physics Laboratories, Harvard University, Cambridge, MA 02138,USA.

[2]Physics Department, Technion, Haifa 32000, Israel.

[3]Department of Physics, Weizmann Institute of Science, Rehovot, Israel.

(Dated: March 23, 2022)

It has been proposed that the microwave-induced "zero-resistance" phenomenon, observed in a GaAs two-dimensional electron system at low temperatures in moderate magnetic fields, results from a state with multiple domains, in which a large local electric field $E(r)$ is oriented in different directions. We explore here the questions of what may determine the domain arrangement in a given sample, what do the domains look like in representative cases, and what may be the consequences of domain-wall localization on the macroscopic dc conductance. We consider both effects of sample boundaries and effects of disorder, in a simple model, which has a constant Hall conductivity, and is characterized by a Lyapunov functional.

PACS numbers:

I. INTRODUCTION

The spontaneous formation of domain patterns is a frequent occurrence in non-equilibrium systems, and it has been extensively studied in fluid systems subject to heating or rotation, in non-equilibrium crystal growth, in driven interfaces between immiscible fluids, in roughness patterns on fracture surfaces, in chemically reacting fluids, in dielectric breakdown, in liquid crystal structures, in nonlinear optics, and in motion of granular materials [1, 2, 3]. In some cases, domain formation is truly an example of spontaneously broken symmetry; i.e., there are two or more domain structures which are equally possible, and selection between them is triggered by thermal noise or some other accident of the history of the sample. In other cases, small perturbations due to frozen-in disorder, peculiarities at the boundaries, or other deviations of the physical system from a symmetric idealized model are responsible. In this paper, we discuss a recently discovered system where spontaneous formation of domains is

believed to occur and to play an important role in macroscopically observable properties, the so-called microwave-induced zero-resistance state in two-dimensional electron systems, in the presence of a moderately-strong magnetic field, at low temperatures.

Experiments on very high mobility two-dimensional electron systems in GaAs heterostructures, in fields ranging from about ten to a few hundred millitesla, have shown large changes in the dc resistance in the presence of microwave radiation, whose sign depends on the ratio $\epsilon = \omega/\omega_c$ between the microwave frequency ω and the cyclotron frequency ω_c [4]. In particular, decreases in the resistance have been observed when ϵ is somewhat larger than the nearest integer. Moreover, in these frequency intervals, if the microwave power is sufficiently high, the resistance can drop by several orders of magnitude, perhaps falling below the experimental sensitivity, whence the designation Zero Resistance State. We note that in the presence of a magnetic field, where there is a nonzero Hall conductance, zero longitudinal resistivity is equivalent to zero longitudinal conductivity: the current is perpendicular to the electric field. Here, we find it more convenient to emphasize the conductivity rather than resistivity. The longitudinal resistance is most directly measured in a Hall bar geometry, whereas the longitudinal conductance is measured in an annular Corbino geometry, illustrated in Fig. 2 below.

Two distinct microscopic mechanisms for conductivity corrections have been proposed: (i) the displacement photocurrent (DP) [5], which is caused by photoexcitation of electrons into displaced guiding centers; and (ii) the distribution function (DF) mechanism, which involves redistribution of intra Landau level population for large inelastic lifetimes [6].

Andreev et. al. [7], have noted that irrespective of microscopic details, once the radiation is strong enough to render the local conductivity negative, the system as a whole will break into domains of photogenerated fields and Hall currents. In the proposed domain phase, motion of domain walls can accommodate the external voltage, resulting in a Zero Conductance State (ZCS) in the Corbino geometry, or a Zero Resistance State for the Hall bar geometry, in apparent agreement with experimental reports [4].

Nevertheless, many questions remain to be answered. What determines the arrangement of domains and domain walls in an actual sample? Is the domain pattern static, or does it evolve periodically or chaotically in time? What are the effects of sample boundaries and inhomogeneities? What do the domain patterns look like in representative cases? If there are favored positions for the domain walls, what effects will this have on the measured

electrical conductance?

We address some of these questions here in the framework of a simple phenomenological model. Further details may be found in a previous publication by the current authors.[8]

II. MODEL.

A. General form

In our model, in the presence of the microwave field, there is a local, non-linear relation between the dc current $j(r)$ and the local electrostatic field $E(r)$:

$$j = j^d(E;r) + j^H(E;r); \tag{1}$$

where j^H is the Hall current and j^d is the dissipative current, defined by the requirements $^d = {}^d$, $^H = {}^H$, where

$$^d(E) \quad @j^d/@E : \tag{2}$$

$$^H(E) \quad @j^H/@E : \tag{3}$$

These equations must be combined with the continuity equation, $r \quad j = \quad _$, where $$ is the charge density, and additional equations that relate the electric field to the charge density.

In our simplest model, we assume that the Hall current is given by a linear relation

$$j^H = {}^H \hat{z} \quad E ; \tag{4}$$

and the Hall conductance ^{H} is assumed to be a constant, independent of position. As we shall see below, there exists a Lyapunov functional[2], which we can use to determine the steady states, the global conductance and stability conditions on domain walls in the strong radiation regime.

The function j^d, in general, will depend explicitly on the position r, due, e.g., to inhomogeneities in the 2D electron system, and the direction of j^d may not be perfectly aligned with E. Equation (1) is valid above an ultraviolet cutoff, which for the system under consideration is probably of the order of the cyclotron radius, of order 1 m.

Writing $E = -\nabla\phi$, we may relate changes in the electrostatic potential ϕ to changes in ρ through the inverse capacitance matrix W:

$$\phi(r) = \int d^2r' W(r,r') \rho(r'). \tag{5}$$

If a time-independent steady state is reached, then we have simply $\nabla \cdot j = 0$, and the precise form of W is unimportant.

In a Corbino geometry, one specifies the potential on the inner and outer boundaries of the sample, and one looks for a solution for $\phi(r)$ consistent with these boundary conditions. If σ_H is a constant, then the Hall current cannot contribute to $\nabla \cdot j$ in the interior of the sample, so it does not appear in Kirchoff's equations. Consequently, the solution for $\phi(r)$ is independent of σ_H, and we may, for simplicity, set $\sigma_H = 0$. To recover the Hall current, one inserts the solution E into the second term in (1).

The symmetry condition on σ_d allows us to define a Lyapunov functional for j_d, as

$$G[\rho] = \int d^2x\, g(E), \quad g = \int_0^{E(x)} dE'\, \sigma_d(E'). \tag{6}$$

A variation of (6) is given by

$$\delta G = \int d^2x\, \nabla\cdot j_d \delta\phi - \int_{\text{bound}} ds\, \hat{n}\cdot j_d \delta\phi \tag{7}$$

The second integral vanishes on equipotential boundaries, or in the absence of external currents. The extrema of G are found to be steady states, with $\nabla \cdot j = 0$. Using the positivity of the inverse capacitance matrix W, one may show that $G[\rho(t)]$ is indeed a Lyapunov functional, i.e. a non-increasing function of time, so that its minima are stable steady states. In general, G may have multiple minima. Any initial choice of $\rho(r)$ will relax to some local minimum of G, but not necessarily the "ground state" with lowest G. Nevertheless, we might expect that the system is most likely to wind up in a state with G close to the absolute minimum, and in the presence of noise, we might expect that the system might tend to escape from high-lying minima.

Using the boundary term in (7), the current across a Corbino sample is equal to the first derivative of G with respect to the potential difference V between two edges, and the conductance is given by the stiffness, or the second derivative:

$$\frac{I}{V} = \frac{d^2G}{d(\delta V)^2}. \tag{8}$$

B. Strong Radiation.

We now consider the clean system ($E_d = 0$) in the regime of strong microwave radiation at positive detuning, i.e., with microwave frequencies slightly larger than the cyclotron harmonics $\omega = m\omega_c$, where $m = 1, 2, \ldots$. Both DP and DF mechanisms produce a regime of negative longitudinal conductivity around $E = 0$, which implies a minimum of $g(E)$ at a finite field of magnitude $E = E_c$. If the radiation is strong enough, E_c can become the global minimum, and the Lyapunov density describes a dynamical phase of spontaneous photogenerated fields. Then g can be expanded as

$$g_0(E) = g_0(E_c) + \frac{1}{2}(E - E_c)^2 \, \epsilon_c + \ldots \qquad |\nabla \cdot E| \qquad (9)$$

where the subscript 0 denotes the absence of disorder. A representative g and the corresponding dissipative current j^d are shown in Figs. 1a and 1b. In order to satisfy equipotential boundary conditions and the constraint $\nabla \cdot E = 0$, domain walls between different directions of E must form. The field derivative coefficient $\epsilon_c l_{dw}^2$ implements the ultra-violet cutoff, giving a finite domain-wall thickness scale l_{dw}. Domain walls give a positive contribution to G of order $\epsilon_c E_c^2 l_{dw}$ per unit length. In the absence of disorder, the system will simply minimize this residual domain wall contribution, subject to aforementioned constraints.

Local stability requires that g is concave near E_c. By rotational symmetry g_0 is a 'Mexican hat' function with a flat valley along $|E| = E_c$. Away from domain walls, the fields are 'marginally' stable. The clean system has zero conductance in the limit when the system size is much larger than l_{dw}. The system can accomodate a potential difference by moving domain walls and by changing the direction of E while keeping $|E| = E_c$, and keeping g_0 constant everywhere away from domain walls. The current density is maintained at zero everywhere, except for possible contributions that vanish in the limit $l_{dw} \to 0$, which is a property of the clean ZCS [7].

III. DOMAIN STRUCTURE IN THE ABSENCE OF DISORDER

Although the Lyapunov cost per unit length of a domain wall depends on the precise angular difference of the orientations of the electric fields on the two sides of it, the pattern of domain walls in the simplest cases, in the absence of disorder, can be understood as an attempt to minimize the total domain wall length, subject to the boundary constraints. If

the potential is a constant, which we may take equal to zero, everywhere along the boundary, we are led to the trial solution:

$$(r) = E_c d(r) \tag{10}$$

where $d(r)$ is the distance to the nearest boundary. The negative of this solution, with E_c replaced by $-E_c$, is an equally good solution, with the same Lyaponov cost. Domain walls for these solutions occur along curves which are the loci of points that are equidistant from two different points on the sample boundary. Domain walls may end, or one domain wall may split into two, at special points, which are equidistant from three different points on the boundary. Some simple examples, illustrating these possibilities, are given in Figs. 2 and 3.

Clearly, the trial solution (10) satisfies the requirement that $E = E_c$ everywhere except on the domain walls. Moreover, the requirement $E = E_c$ requires that in the absence of singularities, two nearby equipotential contours must be separated from each other by a constant distance $$, equal to the difference in the potentials divided by E_c. Thus, if one starts from a point on the sample boundary, the potential (r) must be given by (10) or its negative at least until one encounters a domain wall. If one adds additional domain walls, one may construct solutions different from these, but only by increasing the total length of the domain walls and presumably increasing the Lyapunov cost. Note that one cannot simply displace a domain wall to one side or another without violating the condition $E = E_c$, or introducing a discontinuity in $$ (i.e., an infinite electric field), which we do not allow.

In the circularly symmetric Corbino geometry, illustrated in Fig. 2, we see that if there is no voltage difference between the inner and outer edges, the domain wall must sit at radius $R = R_m$ where R_m is the arithmetic mean of the radii of the inner and outer edges. The domain wall has a Lyapunov cost $G = 2 R g_w$, where g_w is the cost per unit length of a 180-degree domain wall. If the the potential $$ at the outer edge is increased by a small amount V, while the potential at the inner edge is held constant, the position R of the domain wall must change by an amount $R = -V/2E_c$, where the sign depends on which of the two solutions, (10) or its negative, one is starting from. Consequently, since $I = dG/dV$, there should be a small but non-zero photocurrent, $I = -g_w/E_c$ between the outer and inner edges, at $V = 0$.

Non-zero V breaks the perfect degeneracy between the two steady state solutions, as the solution with negative R has the smaller value of G, and it has current in the opposite direction to the voltage drop. If the system can switch from one state to another, the current

will change direction discontinuously when V passes through zero. In the absence of noise, or if V is changed sufficiently rapidly, however, the system may be trapped in one state or the other, in which case there will be no discontinuity at V = 0.

IV. LONG WAVELENGTH DISORDER.

In an inhomogeneous system, there will generally be a non-zero electrostatic field, $E_d(r)$ $r_d(r)$ present in the thermal equilibrium state, with no microwave radiation or bias voltage. (Recall that it is the electrochemical potential, which is the sum of the electrostatic potential and the internal chemical potential, that is constant in equilibrium). We may ask how this disorder field will alter the ZCS.

At weak disorder field, $|E_d| << E_c$, we expand the Lyapunov density in a region where $E \quad E_c$,

$$g(E;E_d) = g_0(E) \quad {}_1(E)E \quad E_d(r) + O(E_d^2); \tag{11}$$

which yields a current density

$$j^d(r) = \quad {}_1E_d + \frac{g_0^0 \quad {}_1^0E \quad E_d}{E}E; \tag{12}$$

where $X^0 \quad @X=@E$, and the coefficient ${}_1$ depends on the microscopic mechanism. A typical g in the presense of disorder is displayed in Fig. 1c. For a simple model based on the displacement mechanism, we estimate that ${}_c$ and ${}_1(E_c)$ should be close to the dark conductivity, while ${}_1^0 \quad {}_c=E_c$. Other models may have quite different values of ${}_1$.

Our use of (11) assumes that the length scale of the disorder field is greater than the domain wall thickness l_{dw}, which is the same as our short wavelength cutoff.[9] In practice, however, we will only be interested in fluctuations on length scales much longer than this. In two dimensions, if the disorder potential ${}_d$ does not have correlations on a length scale much longer than l_{dw}, and if $E_d \; {}_1 \quad E_c \; {}_c$, then the gain in G obtained by aligning E with E_d will be too small to overcome the cost of introducing new domain walls.[8] Then even in the limit of a very large sample, the number and positions of domain walls will be determined by the sample shape and boundary conditions, just as if there were no disorder present. By contrast, if the disorder has correlations which fall off slowly at large distances, then for the model given by (11), with a fixed root-mean-square value of E_d, it will pay to introduce a network of new domain walls, if the sample is sufficiently large, and we would

expect that local characteristics of the domain wall pattern will become independent of the sample size.

A. Stability Conditions.

Stability requires that the local conductivity tensor ^{d}, defined by (12), has non-negative eigenvalues at every point. The lower (transverse) eigenvalue is given by

$$= \frac{g_0^0 \quad {}^0_1 E \quad E}{E} + O(E_d)^2 \quad 0 ; \tag{13}$$

so marginal stability occurs at $E = E_c + {}^0_1 E_d \quad E =_c$.

In a steady state, the normal current density across a domain wall must be continuous. If $\hat{n}$ is the normal, and E_1 and E_2 are the fields on the two sides, we find from (13) and (11) that

$$(E_1) E_1 \hat{n} = \quad (E_2) E_2 \hat{n} + O(E_d^2) \tag{14}$$

When the normal component of E has opposite signs on the two sides, (as occurs in the clean limit), (14) can only be satisfied for $(E_1) = \quad (E_2) = O(E_d)^2$. This restricts the fields at the domain wall to be at their respective marginally stable values. Among the other consequences of these equations, it can be shown that if a path along a set of domain walls forms a closed loop, the integral of the "two-dimensional disorder-charge density" $q_d(r) \quad r \quad _d E=2$, over the area enclosed by the loop, must be equal to zero, up to possible corrections of order E_d^2.[8]

To a lowest order in $\frac{E_d}{E_c}$, the field E will have magnitude E_c within each domain. Coupled with the fact that the parallel component of electric field is continuous across the domain wall, this implies that the domain wall between any two domains is oriented in such a way as to bisect the angle between the field lines of the two domains.

Finally, we note that generically, the differential conductance of a sample in the Corbino geometry can be obtained by solving for the conductance of a linear system with local conductivity given by $^{d}(E(r))$, in series with resistive elements along the domain walls, which arise from movement of the domain walls in response to a variation in the applied bias V. There could also be discontinuities in the current at discrete values of V, if the system jumps discontinuously from one minimum of G to another. We find that for weak

long-wavelength disorder, the scale of the macroscopic conductance is set by the domain-wall contribution.

B. One-Dimensional Disorder.

The simplest example to consider is the case of one-dimensional disorder, where $_d$ is a function of y, independent of the x-coordinate. At wavelengths much larger than l_{dw}, if we do not specify the total voltage drop V, the Lyapunov functional G is minimized if the system breaks up into parallel domains, so that E is everywhere aligned with E_d, and $j^d = 0$. These conditions determine E (y) via (12). They are consistent with the boundary conditions for a rectangular Corbino geometry, which has periodic boundary conditions at $x = 0$ and $x = L$, and specified potentials at $y = 0$ and $y = W$, provided that the voltage difference V satisfies

$$V[I] = \int_0^W dy\,(E^y(y) \quad E_d^y(y)) : \tag{15}$$

Thus, at strong radiation intensity and zero current, we see that that the domain walls form precisely at maxima and minima of $_d$, at positions $y_i; i = 1;::N$, where $E_d^y(y)$ changes sign. For a general choice of $_d(y)$, when no current is drawn from the sample, there will be a non-zero photovoltage, whose value is independent of the magnitude of $_d$, to lowest order, and is determined by the positions y_i :

$$V(j = 0) = E_c \quad (\ 1)^N W \quad 2 \sum_{i=1}^{N} (\ 1)^i y_i \ + O(E_d); \tag{16}$$

where we have assumed that the odd values of i correspond to maxima in $_d$.

If there is a non-zero current j_y^d (in the y-direction), the domain walls will be displaced, leading to a change in voltage proportional to j_y^d. For an appropriate choice of j_y^d, such that the voltage resulting from j_y^d cancels the zero-current photovoltage, we can get $V = 0$. Near $j_y^d = 0$, the differential conductivity $_{yy}$ is given, to lowest order in $_d$, by

$$\frac{1}{_{yy}} = \frac{2E_c}{_1 L} \sum_i \frac{1}{j\,{}_d''(y_i)j} \quad \frac{2E_c}{_1 \tilde{E}_d}: \tag{17}$$

If $P(E_d)$ is the probability distribution for E_d at a random point, it can be shown that $\tilde{E}_d{}^{1} = P(0)$. If E_d is taken from a Gaussian distribution, then $\tilde{E}_d = (2)^{1=2} E_d^{rms}$, where E_d^{rms} is the root-mean square value of E_d. If $_d$ is a single sine wave, then $\tilde{E} = 2^{1=2}\ E_d^{rms}$.

The transverse differential conductivity σ_{xx}, which can also be calculated using (13) and (12), with $j_y^d = 0$, is given, to a first order in σ_d, by $\sigma_{xx} = \sigma_d < |E_d| > / E_c$, where $< |E_d| >$ is the mean value of $|E_d|$. For a gaussian distribution, one has $\sigma_{xx} = (2/\pi)\,\sigma_{yy}$, while for a single sine wave, $\sigma_{xx} = (4/\pi^2)\,\sigma_{yy}$.

In Fig. 4a, we show potentials $\phi(y)$ for the cases $j_y^d = 0$ and $V = 0$, corresponding to a particular choice of the one-dimensional disorder potential $\sigma_d(y)$.

C. Two-Dimensional Disorder Potentials

1. Egg-carton potential

Perhaps the simplest 2D choice for σ_d is the periodic separable egg-carton potential, given by

$$\sigma_d = A \sin(k_x x) + B \sin(k_y y) : \tag{18}$$

We consider here a finite system, a rectangle L_x by L_y, with periodic boudnary conditions on the current and the electric fields. This, of course, is equivalent to considering an infinite system. For bias voltage $V = 0$, we construct a trial solution for ϕ by placing domain walls on the lines $x = \pm(2m+1)/2k_x$ and $y = \pm(2n+1)/2k_y$, for integer n and m. Our trial solution will have a constant electric field in each rectangular domain:

$$E = E_c(-\hat{x}\cos\theta_0 - \hat{y}\sin\theta_0) : \tag{19}$$

Here, θ_0 is the angle between the field and the y axis. Combining equations (11) and (19), we see that, to a linear order, minimization of G is equivalent to maximization of $\int d^2x E_d \cdot E$. The value of G is minimized with the choice $\theta_0 = \arctan(A k_x / B k_y)$. The domain walls satisfy the neutrality condition that $\int q_n(r) d^2r = 0$ in each domain, and the electric field is the gradient of a continuous potential as required.

In the symmetric case, $k_x = k_y; A = B$ $E_d^0 = (2^{1/2} k_x)$; the domain walls form a square array, and $\theta_0 = \pi/4$. We have carried out a numerical minimization of G, and have plotted the "two dimensional charge density", $q(r) \equiv \nabla \cdot E/2\pi$, for the symmetric egg-carton potential, for zero bias voltage in Fig. 5a. Domain walls, appearing here as line singularities, form a square array. Evidently, the numerical solution we obtained is very close to the variatonal one above.

We now construct a variational solution for the case where there is a nonzero voltage drop V along x-direction. Assuming that the electric field is still constant within each domain, we allow the centers of domain walls that are perpendicular to the voltage drop to shift by amount x and rigidly rotate walls through an angle . The electric fields in the various domains will now lie in the directions $(_0 +)$ and $(+ _0)$, so that the domain walls still bisect the angle formed by the field lines in the neighboring domains. In Fig. 5b, we plot the (numerically obtained) "two dimensional charge density", for a bias voltage corresponding to an average electric field equal to $0.25E_c$ in the x direction. The numerical solution is very much like the variational one just described in that domain walls perpendicular to voltage drop are shifted and tilted into a herringbone pattern, while the walls along the voltage drop are essentially unchanged.

The variational solution above can be used to evaluate conductivity $_{xx}$. For a voltage drop V along x-direction, we have

$$\frac{2\ V}{E_c L_x k_x} = 4\ x \sin\ _0 + \frac{2}{k_x}\ \cos _0 : \tag{20}$$

Lyapunov functional G will then be

$$G(V) = G_0 + G_1\ \ \frac{1}{2}(k_x\ x)^2 \sin^2\ _0 + \ ^2\ \ \frac{1}{2} + \frac{^2}{24}\ \ \frac{k_x}{k_y}\ ^2 \sin^2\ _0\ \ \ ! \ ! \ ; \tag{21}$$

where G_0 is the Lyapunov "energy" for the case of $V = 0$ and $G_1 = \frac{2\ _1 E_c L_x L_y}{\sqrt{(A k_x)^2 + (B k_y)^2}}$. Using Eq.20, we minimize the quadratic form above. By taking derivatives of the resulting expression with respect V, as prescribed by Eq.8, we obtain the following expression for $_{xx} = \frac{L_x}{L_y} G''(0)$:

$$_{xx} = \frac{_1}{2}\ \frac{\sqrt{(A k_x)^2 + (B k_y)^2}}{E_c}\ \frac{1 + \frac{^2}{12}\sin^2\ _0\ \ \frac{k_x}{k_y}\ ^2}{1 + \frac{^2}{12}\sin^2\ _0\ \ \frac{k_x}{k_y}\ ^2 + \frac{^2}{4}\cos^2\ _0} : \tag{22}$$

For the symmetric case, this reduces to $_{xx} = 0.83\ _1 E_d^0 / E_c$. As in the 1D case, the conductance is of order $_1 E_d^{rms} / E_c$, reflecting the pinning effect of the "disorder potential" $_d$.

Numerical solutions, referred to above, have been obtained by numerically minimizing the Lyapunov functional. We employ a MATLAB-based routine to minimize the functional, which we discretize on a triangular lattice (typically containing around 14,000 points) in order reduce any perturbations arising from lattice anisotropy. The potential (r) is subject

periodic boundary conditions in the y-direction, and is required to change by a chosen bias voltage V in the x-direction. Having started with a random initial guess for (r), the code allows the potential to relax to a local minimum. The robustness of a minimum, i.e. its "globality", can be ascertained by starting with a different initial guess and/or giving the solution we arrive at random kicks and plugging that in for the next initial guess. As already mentioned, for the case of egg-carton potential, we find that the variational solutions above are quite close to the ones we arrive at via numerics.

2. Disordered case

The numerical routine allows us to obtain solutions for disorder potentials much more complicated than the simple egg-carton potential. For example, in Fig. 4b, we display the self-consistent potential (r) for the case of $_d$ containing 20 Fourier components, chosen from a gaussian distribution with $< j_d(k)j^2 >$ independent of k. The disorder potential $_d$ is also shown. In Fig. 5c, we plot the "two-dimensional charge density", proportional to r E, corresponding to this solution. Domain walls again appear as line singularities in the charge. Although one might expect frustration to reduce the conductance in complicated potentials, the conductivity in this case was found to be similar to that for an egg-carton potential with the same value of E_d^{rms}.

In both the egg carton potential and the more complicated potential of Fig. 4b, there is frustration in the minimization of G. The field E is unable to align perfectly with $E_d(r)$, because of the conflicting requirement of E E, which arises from stability, and r E = 0. Because of this, the dissipative current j^d is generally non-zero, of order $_1E_d$, leading to circulating dissipative currents within each domain. These are indicated by arrows for one domain in Fig. 5c. The much larger circulating Hall currents, of magnitude $^H E_c$, are not shown in the figures.

V. DISCUSSION.

In this paper, we have explored the effects of sample boundaries and long-wavelength potential disorder, on the domain pattern and conductance of the microwave-induced zero-resistance state, within a simple model. In particular, our model, with a constant Hall

conductance, has the simplifying feature that it has a Lyapunov functional. In considering the effects of disorder, we assumed a linear coupling to the disorder-induced electrostatic field E_d. Furthermore, while we consider non-linear effects due to the self-consistent electric field E, we do not consider non-linearities due to changes in the local electron-density itself, which may result from the electric fields of the domains. (We might expect density fluctuations to be small, while potential fluctuations are large, if the system is far from any screening conductors.) For more complicated systems, where there is no Lyapunov functional, we do not even know whether the system will reach a time-independent steady state, in the presence of strong microwave radiation.

Even for our simple model, with its Lyapunov functional G, there are many questions to be answered. What actually is the behavior of a system with two-dimensional disorder, in the limit of a large system size? Will there be a large number of metastable steady states, as in a glass, with associated hysteresis in the observed current/voltage curve? If we assume that for all values of the potential difference V between the inner and outer edge, in the Corbino geometry, the system can reach the state with lowest value of G, will the conductance be finite in the limit of large system size, with magnitude of disorder held fixed, or will it, perhaps, go to zero in this limit?

Experimental work in the field is also in its infancy. The self-consistent electrostatic potential (r) generated by the domains can in principle be measured with minimal disturbance of the sample, using, for example, a single electron transistor device. Such a method has been used successfully to explore various aspects of the microscopic properties of the integer and fractional quantum Hall effect[10], and we may expect important information about domain structures to come from such measurements in the future.

We remark that Alicea et al.[11] have shown that a Lyapunov functional exists, rather generally, very close to the dynamical phase transition, where the microwave power is such that the longitudinal conductivity first becomes negative at $E = 0$. However, the form of their functional is different from the one employed in the present paper. We are interested here in systems under strong microwave irradiation, far from the phase transition, so the Lyapunov functional of Alicea et al does not apply.

Acknowledgments. We thank M. Lukin, S. Fishman, E. Meron, and Y. Yacoby for helpful discussions. Work was supported in part by the Harvard Center for Imaging and Mesoscale Structures, NSF grant DMR 02-33773, US-Israel Binational Science Foundation,

Minerva Foundation and the DFG priority program on Quantum Hall Systems YA 111/1-1. One of the authors, AA, would also like to acknowledge the hospitality of Aspen Center for Physics.

---

[1] J. P. Gollub and J. S. Langer, Rev. Mod. Phys. 71, S396 (1999).

[2] M. C. Cross and P. C. Hohenberg, Rev. Mod. Phys. 65, 851 (1993).

[3] J. S. Langer, Rev. Mod. Phys. 52, 1 (1980).

[4] R. G. Mani, J. H. Smet, K. von Klitzing, V. Narayanamurti, W. B. Johnson, V. Umansky, Nature, 420, 646 (2002); M. A. Zudov, R. R. Du, L. N. Pfeiffer, K. W. West, Phys. Rev. Lett. 90, 046807 (2003); C. L. Yang, M. A. Zudov, T. A. Knuuttila, R. R. Du, L. N. Pfeiffer, K. W. West, Phys. Rev. Lett. 91, 096803 (2003); R. L. Willett, L. N. Pfeiffer, K. W. West, Phys. Rev. Lett. 93, 026804 (2004).

[5] V. I. Ryzhii, Fiz. Tverd. Tela 11, 2577 (1969) [Sov. Phys. Solid State 11, 2078 (1970)]; A. Durst, S. Sachdev, N. Read, and S. M. Girvin, Phys. Rev. Lett. 91, 086803 (2003); P. W. Anderson and W. F. Brinkman, cond-mat/0302129; J. Shi and X. C. Xie, Phys. Rev. Lett. 91, 086801.

[6] I. A. Dmitriev, A. D. Mirlin and D. G. Polyakov, Phys. Rev. Lett. 91, 226802 (2003); I. A. Dmitriev, M. G. Vavilov, I. L. Aleiner, A. D. Mirlin and D. G. Polyakov, Phys. Rev. B 71, 115316 (2005).

[7] A. V. Andreev, I. L. Aleiner, and A. J. Millis, Phys. Rev. Lett. 91, 056803 (2003); M. G. Vavilov and I. L. Aleiner, Phys. Rev. B 69, 035303 (2004).

[8] A. Auerbach, I. Finkler, B. I. Halperin, and A. Yacoby, Phys. Rev. Lett. 94, 196801 (2005).

[9] Effects of a periodic potential with wavelength shorter than the cyclotron radius have been discussed by J. Dietel, L. I. Glazman, F. W. J. Hekking, F. von Oppen, Phys. Rev. B 71, 045329 (2005).

[10] S. Ilani, J. Martin, E. Teitelbaum, J. H. Smet, D. Mahalu, V. Umansky, A. Yacoby, Nature 427, 328 (2004); J. Martin, S. Ilani, B. Verdene, J. H. Smet, V. Umansky, D. Mahalu, D. Schuh, G. Abstreiter, and A. Yacoby, Science 305, 980 (2004).

[11] J. Alicea, L. Balents, M. P. A. Fisher, A. Paramekanti, L. Radzihovsky, Phys. Rev. B 71, 235322 (2005).

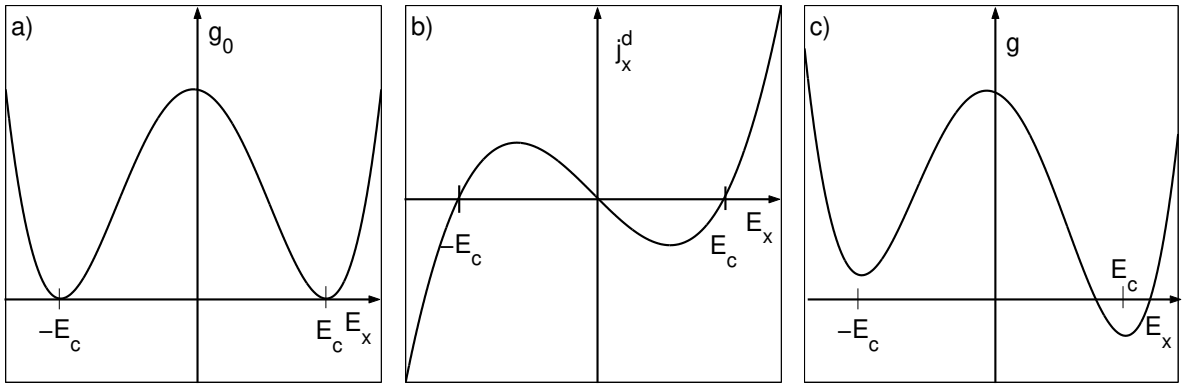

FIG. 1: Model Lyapunov functions g and dissipative current j_x^d for a uniform electrostatic field E_x along the x-axis ($E_y = 0$), in the presence of strong microwave irradiation. (a) Lyapunov function $g_0(E_x)$ in the absence of disorder. Operating points are at the minima of g, where $E_x = \pm E_c$. (b) Dissipative current corresponding to g_0. The dissipative current, parallel to E, vanishes at the operating points $E_x = \pm E_c$. There will be a non-zero Hall current in the y-direction. (c) Lyapunov function in the presence of a uniform disorder field E_d in the x-direction.

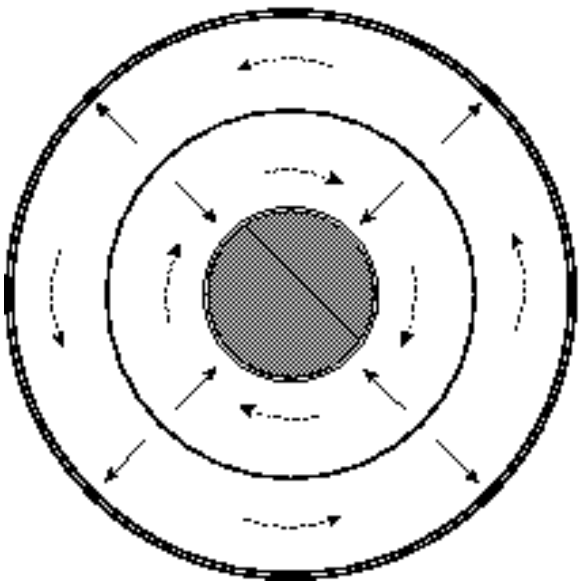

FIG. 2: Domain structure for a circularly-symmetric Corbino geometry, in the macroscopic limit, without disorder. Solid circle, midway between the inner and outer edges is the location of the domain wall when there is no voltage difference between the two edges. Solid arrows show the direction of the electrostatic field E, while dotted arrows show the direction of the circulating Hall currents. An alternate solution of the equations has the same position of the domain wall, but reversed directions for the electric fields and Hall currents. In a Corbino conductance measurement, one applies a voltage difference between the inner and outer edges, and measures the electrical current from one edge to the other.

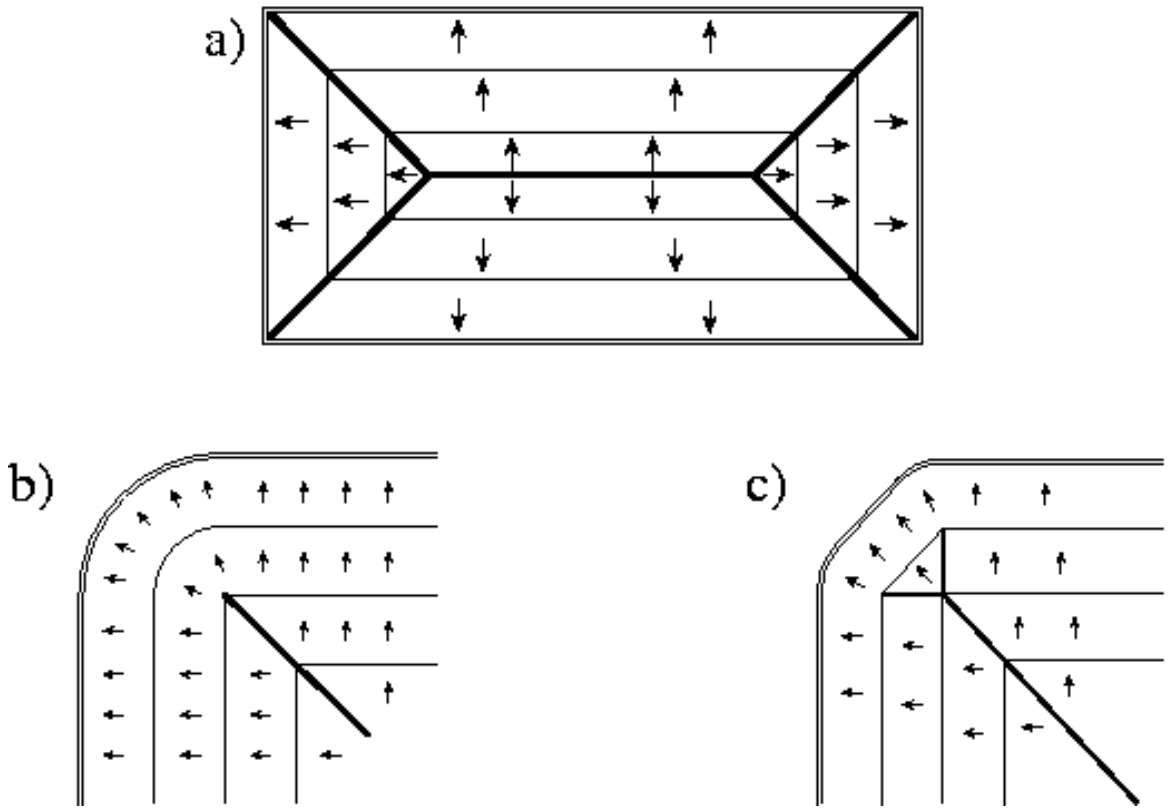

FIG. 3: Other possible domain structures in a sample without disorder. Heavy solid lines show domain walls; light solid lines show representative equipotential contours; and double lines show sample boundaries. Arrows show direction of electric field E. Panel (a) shows structure for a rectangular sample. Panel (b) shows how a domain wall can end inside the sample, in the vicinity of a curved corner. Panel (c) shows how a domain wall can split into two.

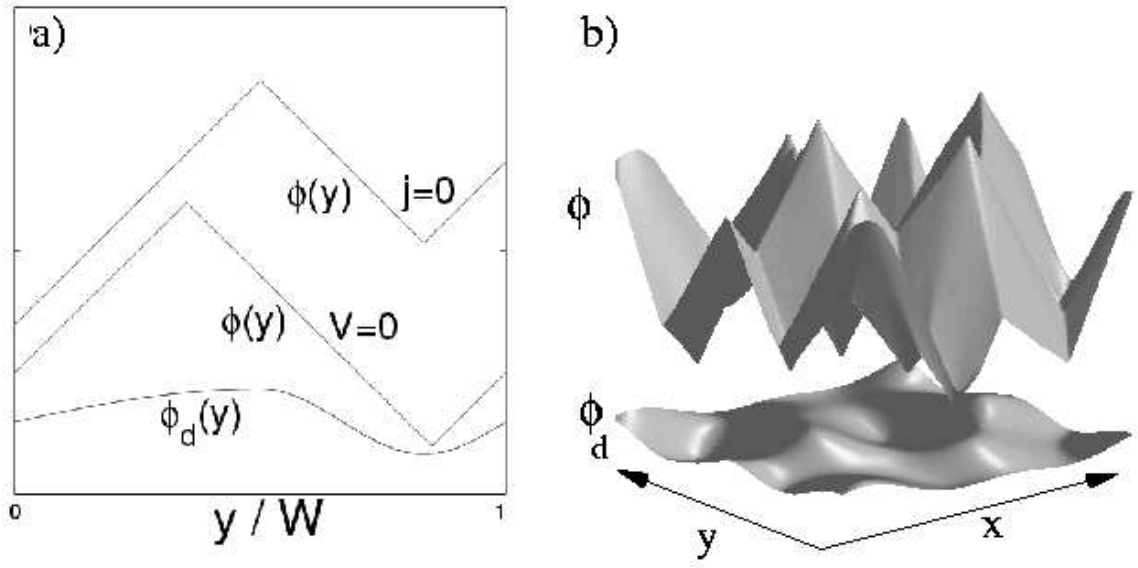

FIG. 4: Examples of a disorder potential $_d(r)$ and the resulting self-consistent potential (r). Different vertical scales were used for and $_d$. Panel (a) shows an example of one-dimensional disorder, where $_d$ and depend only on the coordinate y. Solutions are shown for two different boundary conditions, corresponding to zero net voltage drop and to zero longitudinal current flow. Panel (b) shows (r) resulting from a particular two-dimensional disorder potential $_d$, indicated in the lower plot. The disorder potential contains 20 Fourier components, whose amplitudes were chosen from Gaussian distributions with variance independent of the wave-vector k. Periodic boundary conditions were imposed on and $_d$.

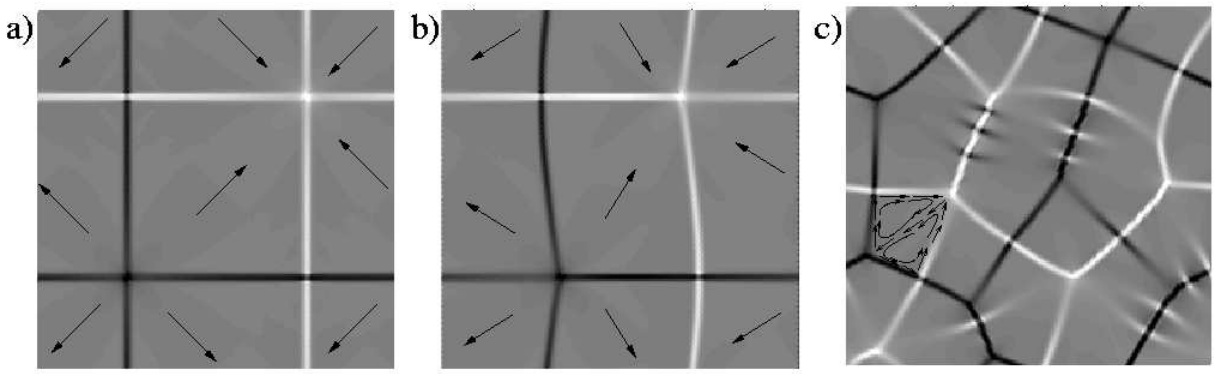

FIG. 5: Gray-scale plots of the "two-dimensional charge density" q(r) r E=2 , for three examples discussed in the text. Domain walls are visible as line singularities in the charge density. Panel (a) shows q(r), in one unit cell, when $_d$ is the periodic symmetric egg-carton potential, $_d$ / cosx + cosy, with zero net voltage drop across the sample. The arrows show the direction of electric eld within each domain. Panel (b) shows q(r) for the same choice of $_d$, with a non-zero voltage bias, corresponding to an average electric eld E = 0:25E$_c$ in the x-direction. Once again, the arrows show the direction of eld within each domain. Panel (c) shows q(r) for the more complicated example of and $_d$ illustrated in Fig. 4b. Arrows here show circulating dissipative currents in one domain.